Author Manuscript

Author Manuscript

Author Manuscript

Author Manuscript

HHS Public Access

Author manuscript

Cell Rep. Author manuscript; available in PMC 2019 April 23.

Published in final edited form as:

Cell Rep. 2019 March 19; 26(12): 3323–3335.e4. doi:10.1016/j.celrep.2019.02.076.

DBC1 Regulates p53 Stability via Inhibition of CBP-Dependent p53 Polyubiquitination

Oluwatoyin E. Akande[1,2], **Priyadarshan K. Damle**[1,2], **Marius Pop**[3], **Nicholas E. Sherman**[4], **Barbara B. Szomju**[1,2], **Larisa V. Litovchick**[1,2], and **Steven R. Grossman**[1,2,5,*]

[1]Department of Internal Medicine, Virginia Commonwealth University (VCU), Richmond, VA, USA

[2]VCU Massey Cancer Center, VCU, Richmond, VA, USA

[3]Kronos Bio, Inc., Cambridge, MA, USA

[4]W.M. Keck Biomedical Mass Spectrometry Laboratory, University of Virginia, Charlottesville, VA, USA

[5]Lead Contact

SUMMARY

The control of p53 protein stability is critical to its tumor suppressor functions. The CREB binding protein (CBP) transcriptional co-activator co-operates with MDM2 to maintain normally low physiological p53 levels in cells via exclusively cytoplasmic E4 polyubiquitination activity. Using mass spectrometry to identify nuclear and cytoplasmic CBP-interacting proteins that regulate compartmentalized CBP E4 activity, we identified deleted in breast cancer 1 (DBC1) as a stoichiometric CBP-interacting protein that negatively regulates CBP-dependent p53 polyubiquitination, stabilizes p53, and augments p53-dependent apoptosis. TCGA analysis demonstrated that solid tumors often retain wild-type p53 alleles in conjunction with DBC1 loss, supporting the hypothesis that DBC1 is selected for disruption during carcinogenesis as a surrogate for p53 functional loss. Because DBC1 maintains p53 stability in the nucleus, where p53 exerts its tumor-suppressive transcriptional function, replacement of DBC1 functionality in DBC1-deleted tumors might enhance p53 function and chemosensitivity for therapeutic benefit.

Graphical Abstract

This is an open access article under the CC BY-NC-ND license (http://creativecommons.org/licenses/by-nc-nd/4.0/).

*Correspondence: steven.grossman@vcuhealth.org.

AUTHOR CONTRIBUTIONS

O.E.A. performed and analyzed the experiments and wrote the manuscript. P.K.D. generated plasmids, B.B.S. generated shRNA stable cell lines. N.E.S. performed MudPIT, and L.V.L. assisted in MudPIT analysis. S.R.G. supervised the study and critically revised the manuscript.

SUPPLEMENTAL INFORMATION

Supplemental Information can be found with this article online at https://doi.org/10.1016/j.celrep.2019.02.076.

DECLARATION OF INTERESTS

The authors declare no competing interests.

Author Manuscript
Author Manuscript
Author Manuscript
Author Manuscript

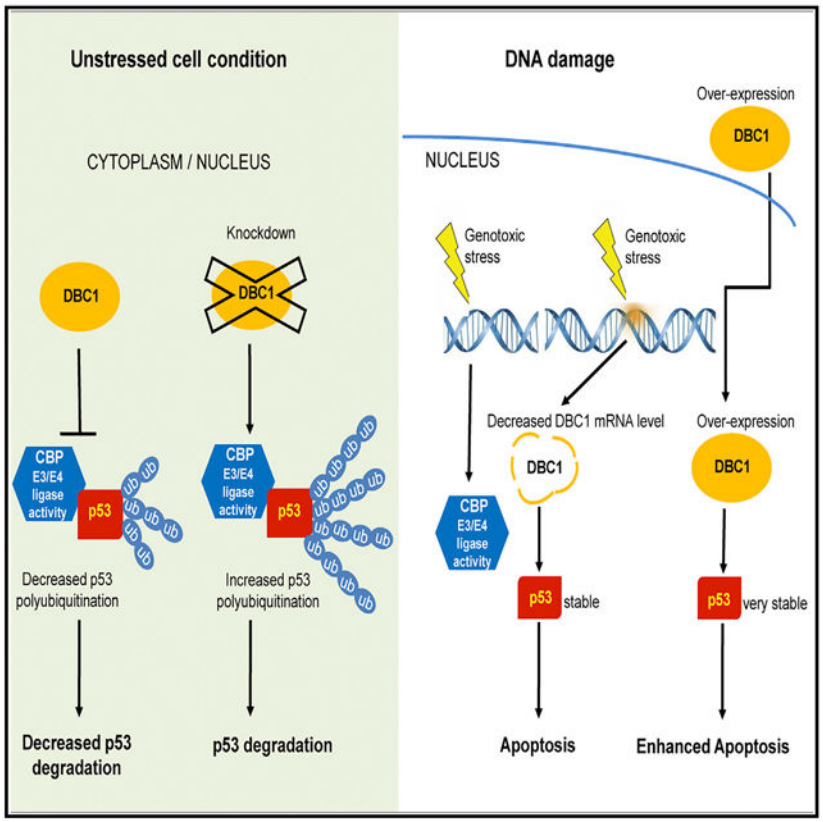

In Brief

Akande et al. describe DBC1 as a negative regulator of CBP p53-directed ubiquitin ligase activity that maintains nuclear p53 stability. DBC1 loss may be selected in tumors to inactivate the p53 pathway. Because expression of DBC1 enhances p53-dependent apoptosis, restoration of DBC1 in null tumors may be of therapeutic value.

INTRODUCTION

The CREB binding protein (CBP) global transcriptional coactivator (Chrivia et al., 1993; Martinez-Balbás et al., 1998) and its paralog p300 encode intrinsic histone acetyltransferase (HAT) activities, acetylating histones at the promoter regions of target genes (Bannister and Kouzarides, 1996; Ogryzko et al., 1996; Chan and La Thangue, 2001) and non-histone proteins, thereby promoting their transcriptional activation (Lill et al., 1997; Vervoorts et al., 2003). Both CBP and p300 participate in various complex pathological and physiological cellular processes, such as cell growth and differentiation, cell transformation and development, response to stress, cell-cycle regulation, and apoptosis (Goodman and Smolik, 2000; Turnell et al., 2005; Turnell and Mymryk, 2006; Arany et al., 1996; Dietze et al., 2005).

CBP-p300 directly contribute to the mechanisms that regulate the stability of p53, a frequently mutated tumor suppressor protein found in many human cancers, whose activity is controlled by covalent post-transcriptional modifications such as acetylation, methylation,

Author Manuscript Author Manuscript Author Manuscript Author Manuscript

phosphorylation, ubiquitination, neddylation, and sumoylation (Symonds et al., 1994; Bode and Dong, 2004; Brooks and Gu, 2003). In the absence of cellular stress, physiological levels of p53 are primarily maintained by ubiquitination activities mediated by its negative modulator, the mouse double minute protein 2 (MDM2), a well-characterized ubiquitin E3 ligase enzyme, in conjunction with CBP-p300, which function as ubiquitin E4 conjugation factors (Li et al., 2003; Brooks et al., 2004; Grossman et al., 2003; Shi et al., 2009). E4 enzymes catalyze ubiquitin chain assembly on preformed ubiquitin moieties of substrates, designating them for 26S proteasomal degradation (Koegl et al., 1999). Early studies have indicated that MDM2 catalyzes multiple monoubiquitination of p53, a signal for p53 nuclear export (Li et al., 2003; Brooks et al., 2004). We previously demonstrated that CBP and p300 encode cytoplasmic-intrinsic, but not nuclear-intrinsic, E4 activities and that the exported monoubiquitinated p53 is polyubiquitinated by cytoplasmic CBP-p300, targeting p53 for 26S proteasomal degradation (Grossman et al., 2003; Shi et al., 2009). However, the mechanism for regulation of the compartmentalized CBP and p300 ubiquitin ligase activities has not yet been examined.

Conversely, in response to cellular stress, mechanisms such as MDM2 inactivation, ataxia telangiectasia mutated (ATM) or ATR-mediated phosphorylation of p53, and acetylation of specific lysine residues in the C-terminal region of p53 by CBP-p300 collectively increase the DNA binding ability, stability, and transcriptional activation of p53 (Turnell et al., 2005; Ferreon et al., 2009; Saito et al., 2003; Grossman, 2001). CBP and p300 thus play dual roles in p53 regulation, promoting p53 polyubiquitination and degradation in the absence of cellular stress (Grossman et al., 2003; Shi et al., 2009) and promoting p53 stability and transactivation in response to cellular insults (Saito et al., 2003; Grossman, 2001).

In this work, we determined the regulation of the compartmentalized ubiquitin ligase activities of CBP. Using Multidimensional Protein Identification Technology (MudPIT) analysis, we identified nuclear and cytoplasmic CBP binding partners. We report that DBC1 is a CBP-interacting partner, with its N terminus binding both N- and C-terminal regions of CBP. Furthermore, our data suggest that DBC1 suppresses nuclear p53 ubiquitination via its interaction with CBP in the nucleus. Loss of DBC1 during genotoxic stress physiologically dampened apoptotic responses to cisplatin due to activation of nuclear CBP E4 activity for p53 with DBC1 loss, and restoration of DBC1 expression heightened cisplatin cytotoxicity. Using The Cancer Genome Atlas (TCGA) database (Gao et al., 2013; Cerami et al., 2012), we found that DBC1 deletion was generally associated with retention of wild-type p53 in several tumors, suggesting DBC1 loss may be selected by tumors as a means of p53 pathway disruption. Altogether, our findings collectively provide insight as to how the CBP-DBC1 interaction participates in the p53 regulatory network, and disruption of DBC1 function in regulating CBP ubiquitin ligase activity toward p53 may be a factor in driving carcinogenesis in tumors that retain wild-type p53 status.

RESULTS

Identification of Nuclear and Cytoplasmic CBP-Interacting Proteins

To define the regulation of compartmentalized CBP ubiquitin ligase activities, we first determined whether CBP-interacting activators or inhibitors of CBP’s ubiquitin ligase

Author Manuscript Author Manuscript Author Manuscript Author Manuscript

activities were present in the cytoplasmic or nuclear fractions, respectively, of U2OS osteosarcoma cells, in which CBP's ubiquitin ligase function had initially been characterized (Grossman et al., 2003; Shi et al., 2009). CBP was immunoprecipitated from cytoplasmic and nuclear fractions of U2OS cells, and nuclear CBP immunoprecipitations (IPs) incubated with either cytoplasmic lysates (lysates before IP) or CBP immunodepleted cytoplasmic lysates (i.e., supernatant obtained post-cytoplasmic CBP IP), followed by *in vitro* CBP E3 autoubiquitination assay (Shi et al., 2009), performed on the washed nuclear CBP IPs (Figures 1A and S1). In this assay, the washed CBP IP is incubated with ubiquitin enzymes E1, E2 (ubc5a), ubiquitin, and ATP, and the products of substrate-independent ubiquitination and/or autoubiquitination are immunoblotted with ubiquitin antibody. Similarly, cytoplasmic CBP IPs were incubated with nuclear lysates or CBP immunodepleted nuclear lysates, followed by *in vitro* CBP E3 autoubiquitination assay performed on the washed cytoplasmic CBP IPs. A CBP-interacting nuclear factor, i.e., a factor removed with CBP immunodepletion, inhibited the *in vitro* CBP E3 autoubiquitination activity of cytoplasmic CBP, while a cytoplasmic factor not depleted by a CBP IP appeared to promote nuclear CBP E3 autoubiquitination activity (Figures 1A and S1).

Next, we sought to identify the CBP-interacting nuclear inhibitor of CBP ubiquitin ligase activities. Using MudPIT proteomic analysis (Yates et al., 2009), we identified CBP-interacting proteins from nuclear and cytoplasmic fractions of U2OS cells. Silver staining of anti-CBP versus control immunoglobulin G (IgG) IPs revealed nuclear CBP was approximately 3-fold more abundant than cytoplasmic CBP, consistent with findings by immunoblots and immunofluorescence (Figures 1B and 1C) (Chrivia et al., 1993). We identified 70 cytoplasmic CBP binding proteins and 48 nuclear CBP binding proteins shared between two independent experiments, with 14 CBP binding proteins found in both compartments in both experiments (Figure 1D). Of particular interest among the identified binding proteins, due to its known connection to p53 stability regulation, was a 130 kDa protein (Figure 1B, in block arrow), with a total spectra count second only to that of CBP in the nuclear fraction and third to CBP's count in the cytoplasmic fraction (Figures 1C and 2A), identified as cell cycle and apoptosis regulator protein 2 (CCAR2), otherwise known as deleted in breast cancer 1 (DBC1) (Hamaguchi et al., 2002).

DBC1 Stably Associates with CBP in Cells

DBC1 was initially mapped to a region homozygously deleted from certain human breast cancers (Hamaguchi et al., 2002; Kim et al., 2009), and it is known to modulate the activities of nuclear receptors (Koyama et al., 2010; Chini et al., 2013) and epigenetic modifiers (Zhao et al., 2008; Chini et al., 2010; Li et al., 2009). MudPIT data revealed 3-fold higher abundance of nuclear DBC1 than cytoplasmic DBC1 from the respective CBP IPs (Figure 2A). To confirm that DBC1 interacts with CBP, we transfected U2OS cells with full-length FLAG-CBP and full-length myc-DBC1 and performed anti-FLAG IPs. myc-DBC1 was detected in the FLAG IP when the two proteins were co-transfected, but not in control dropout IPs (Figure 2B). We further validated the interaction between endogenous CBP and DBC1 by IP of U2OS cell lysates, in which robust co-immunoprecipitation (coIP) with each antibody was observed in both nuclear and cytoplasmic lysates, but no signal was seen in control IgG IPs (Figure 2C, left). Similar evidence of interaction between endogenous CBP

Author Manuscript Author Manuscript Author Manuscript Author Manuscript

and DBC1 was observed in H1299 lung cancer cells (Figure 2C, right). Complementing coIP data, both CBP and DBC1 co-localized in the nucleus by immunofluorescence in 2 disparate cell lines—U2OS (p53 wild-type) and H1229 (p53 null) cells—because that is where the bulk of each protein is localized (Figures 2D and S2).

Retention of Wild-Type p53 in DBC1-Deleted Human Tumors

Next, we queried the TCGA database for *DBC1* cross-cancer alteration in relation to genomic p53 status. Approximately 30% of breast cancer, 40% of lung cancer, and 96% of prostate cancer cases with *DBC1* deletion maintained wild-type genomic p53 (*TP53*) status (Figure 2E). Furthermore, approximately 80% of breast cancer, 60% of lung cancer, and 98% of prostate cancer cases with *DBC1* deletion and wild-type p53 status also maintained wild-type *CREBP* (CBP), *MDM2*, and *CDKN2A* genes, all of which are key factors in the p53 degradation pathway (Figure 2F). These TCGA data suggest the possibility of tumors using *DBC1* loss or inactivation as a means of down-regulating the p53 network, akin to other p53 network alterations, such as loss of p14/p19ARF or MDM2 amplification. Based on the robust CBP-DBC1 interaction, and the association between DBC1 loss and maintenance of wild-type p53, we pursued further detailed analysis of CBP-DBC1 interaction and the role of DBC1 in p53 activity and degradation.

CBP-DBC1 Interaction Depends on the N Terminus of DBC1 and Both N- and C-Terminal Regions of CBP

To identify the regions of DBC1 that are necessary for the CBP-DBC1 interaction, we transfected U2OS cells with full-length FLAG-CBP and truncation mutants of myc-DBC1 (Figure 3A), followed by anti-FLAG IP and FLAG and myc immunoblotting. We found that deletion of the N-terminal 697 amino acids of DBC1 (DBC1(698–923 aa)) abolished the binding between DBC1 and CBP (Figure 3B), while the first 240 amino acids of DBC1 were sufficient for CBP-DBC1 interaction (Figures 3A and 3B). To identify the region or regions of CBP that interact with DBC1, we transfected U2OS cells with full-length myc-DBC1 and N- and C-terminal deletion constructs of FLAG-CBP, followed by anti-FLAG IP and FLAG and myc immunoblotting (Figures 3A–3C). CBP encodes three conserved (with p300) cysteine-histidine-rich domains: CH1 (TAZ1), CH2, and CH3 (TAZ2) located at the N terminus transactivation region, the centrally located acetyl-transferase region, and the C terminus transactivation region, respectively. The tested CBP deletion constructs deleted all 3 domains by C-terminal truncation (1–200 and 1–351), included CH1 (TAZ1) only (1–456 and 1–616), or included CH2 and CH3 only (del 1–665). Myc-DBC1 bound all tested FLAG-CBP constructs, but not to the beads in the control IP (using vector + myc-DBC1 transfection), indicating that DBC1 interacts with both N-terminal and C-terminal domains of CBP (Figure 3C).

DBC1 Regulates Nuclear CBP Autoubiquitination Activity

Based on our observation that DBC1 binds both N- and C-terminal regions of CBP (Figure 3C), we investigated whether DBC1 plays a role in the regulation of CBP ubiquitin ligase activities, which require CBP N-terminal sequences (Shi et al., 2009). U2OS cells were treated with either control small interfering RNA (siRNA) or DBC1 siRNA, followed by CBP IP of cytoplasmic and nuclear lysates and *in vitro* analysis of CBP E3

Author Manuscript Author Manuscript Author Manuscript Author Manuscript

autoubiquitination activity (Shi et al., 2009). As shown in Figures 3D and 3E, downregulation of DBC1 by siRNA led to a surprising and significant increase in nuclear CBP E3 autoubiquitination activity when compared with the effect of control siRNA. In the cytoplasmic fraction, however, the change in CBP autoubiquitination activity in DBC1-depleted cells was subtle when compared with control siRNA (Figures 3D and 3E). Thus, our data suggest that DBC1 behaves similarly to the CBP-interacting nuclear inhibitor identified in Figure 1.

DBC1 Regulates p53-Directed CBP E4 Ubiquitin Ligase Activity

Because we found that DBC1 inhibits CBP E3 nuclear autoubiquitination activity, we examined whether DBC1 also regulates p53-directed CBP E4 (substrate-specific polyubiquitin chain extension) ligase activity. First, we determined the effect of CBP, DBC1, or combined CBP-DBC1 depletion on p53 stability. U2OS cells transiently expressing control, CBP, DBC1, or CBP-DBC1 siRNAs were treated with cycloheximide for 90 min, followed by p53, CBP, and DBC1 immunoblotting. As expected, CBP depletion using siRNA led to increased p53 half-life (>100 min) compared with control siRNA-treated U2OS cells (70 min), consistent with our previous data (Shi et al., 2009) (Figures 4A–4C). DBC1 depletion led to a decrease in p53 half-life (<60 min) compared with control siRNA treatment, while depletion of both CBP and DBC1 rescued the decreased p53 half-life observed in DBC1-depleted cells to >100 min (Figures 4A–4C). Similar results were observed with the MCF-7 breast cancer cell line (Figure S3).

Next, we examined endogenous p53 polyubiquitination in the cytoplasmic and nuclear compartments of cells treated with control, CBP, DBC1, or CBP-DBC1 siRNAs, followed by p53 IP and immunoblotting with p53 and ubiquitin antibodies. DBC1 depletion caused a modest increase in p53 polyubiquitination in the cytoplasmic compartment but a more robust increase in p53 polyubiquitination in the nuclear compartment (where p53 polyubiquitination is absent at baseline) when compared with control siRNA-treated cells (Figures 4D and 4E). As expected, CBP depletion led to a decrease in cytoplasmic p53 polyubiquitination when compared with control siRNA-treated cells, with no effect on nuclear p53 ubiquitination, which remained absent (Figures 4D and 4E). Consistent with CBP's E4 role for p53 polyubiquitination (Shi et al., 2009), CBP-DBC1 double knockdown rescued the increase in p53 polyubiquitination observed in DBC1-depleted cells in both cytoplasmic and nuclear compartments (Figures 4D and 4E). Thus, DBC1 not only blocks CBP E3 autoubiquitination activity but also blocks substrate (p53)-directed CBP E4 activity.

To verify whether DBC1 siRNA inhibition of CBP E4 polyubiquitin activity toward p53 reflects on-target activity, U2OS cells stably expressing DBC1 short hairpin RNA (shRNA) were rescue transfected with either empty vector or shRNA-resistant DBC1(1–470)*, which is competent for CBP binding (Figure 3B). 48 h post-transfection, cells were either harvested for p53 IPs from cytoplasmic and nuclear fractions, followed by immunoblotting with anti-ubiquitin antibody to examine p53 polyubiquitination (Figures 5A, 5C, and 5D), or treated with cycloheximide over a 90-min time course to determine p53 half-life (Figures 5E–5H). Consistent with DBC1's inhibitory action on CBP E3-E4 functions, expression of DBC1(1–470)* reversed the increase in p53 polyubiquitination observed in both nuclear and

Author Manuscript Author Manuscript Author Manuscript Author Manuscript

cytoplasmic fractions of DBC1-depleted cells (Figure 5A). We also found that expression of DBC1(1–470)* in both cytoplasmic and nuclear cell compartments of DBC1-depleted cells led to a drastic increase in p53 half-life (>90 min versus 30–40 min) when compared with DBC1-depleted cells, DBC1-depleted cells transfected with empty vector, or cells expressing control shRNA (Figures 5E–5H). By contrast, when U2OS cells stably expressing DBC1 shRNA were transfected with a non-CBP-interacting DBC1 construct, DBC1(698–923) (Figure 3B), there was no decrease in p53 polyubiquitination as was seen with a CBP-interacting DBC1 construct (Figure 5B). These results indicate that DBC1 inhibits CBP E4 polyubiquitin ligase activity toward p53 in a manner dependent on specific interaction, leading to p53 stabilization, and can do so in both compartments, with the greatest effect in the nucleus, because most DBC1 localized to the nucleus versus cytoplasm (Figure 2).

CBP and DBC1 Play Opposing Roles in Regulating Genotoxin-Induced p53 Ubiquitination and Apoptosis

Given p53's central role in the DNA damage response, both in tumor suppression and in cancer therapy, we investigated whether DBC1's stabilizing effect toward p53 influenced the cellular response to genotoxins, specifically the apoptotic response. First, we examined cytoplasmic versus nuclear p53 ubiquitination in response to genotoxin and stress agent treatment in U2OS cells. Previous work has shown that genotoxins generally stimulate total cellular p53 polyubiquitination at later time points of treatment (6–24 h), and our prior work showed specific accumulation of polyubiquitinated p53 in chromatin but did not examine cytoplasmic p53 ubiquitination (Kaur et al., 2007). Analysis of cytoplasmic and nuclear p53 ubiquitination by p53 IP and ubiquitin immunoblotting of nuclear and cytoplasmic fractions after doxorubicin treatment revealed that nuclear p53 ubiquitination increased, consistent with prior reports (Kaur et al., 2007), while cytoplasmic p53 ubiquitination was unchanged (Figure 6A). The identity of the ubiquitinated bands as p53-ubiquitin conjugates in Figure 6A was confirmed by performing the same experiment using fractions from U2OS cells also treated with scrambled or p53 siRNA, where the p53 IPs from p53 siRNA-treated cells were devoid of any signal in the ubiquitin immunoblot (Figures S4A and S4B).

The effect of doxorubicin on nuclear versus cytoplasmic p53 ubiquitination was mirrored by an analysis of CBP E3 autoubiquitination activity after doxorubicin, etoposide, or ionizing radiation, which revealed 2- to 3-fold induction ($p < 0.05$) of nuclear CBP E3 activity, with no effect on cytoplasmic CBP E3 activity (Figure S5). Accompanying the observed increased nuclear p53 ubiquitination and CBP E3 activity, cisplatin, doxorubicin, and the non-genotoxic stress agent staurosporine caused a sharp and surprising decrease in nuclear, but not cytoplasmic, DBC1 protein levels, concomitant with decreased nuclear CBP-DBC1 interaction as assessed by CBP-DBC1 coIP (Figures 6B and 6C). To investigate the basis of this finding, we examined DBC1 mRNA level post-genotoxic (doxorubicin) and non-genotoxic (staurosporine) stresses. We found a very significant decrease in DBC1 mRNA (and protein) levels at 6 h, but not 1 h, post-doxorubicin and post-staurosporine treatments when compared with untreated cells (Figures 6D and S4C). Furthermore, a decrease in DBC1 nuclear localization was observed by immunofluorescence (Figure 6E); this effect of

Author Manuscript Author Manuscript Author Manuscript Author Manuscript

stress on nuclear DBC1 levels might therefore explain the observed rise in nuclear p53 ubiquitination after stress.

Next, we examined the effect of CBP, DBC1, or CBP-DBC1 depletion on genotoxin-induced apoptosis. U2OS cells stably expressing control, CBP, DBC1, or CBP-DBC1 shRNAs were treated with cisplatin, and apoptosis was measured by flow cytometry for caspase-3 cleavage. After platinum treatment, we observed a consistent but non-statistically significant reduction in cleaved caspase-3 in DBC1-depleted cells when compared with control shRNA-expressing cells (Figure 6F). In contrast, a significant number of cells were labeled with cleaved caspase-3 antibody after both CBP and CBP-DBC1 depletion (Figure 6F). Similarly, immunoblotting for poly-(ADP) ribosyl polymerase (PARP) and caspase-3 cleavage using the same conditions (Figure 6G), or when cells were treated with doxorubicin (Figure S6A), showed a slight decrease in cleaved PARP and caspase-3 in DBC1-depleted cells when compared with control cells and an upregulation of cleaved PARP and cleaved caspase-3 in CBP-depleted cells and double CBP-DBC1-depleted cells (Figures 6G and S6A). These results indicate that DNA damage induces nuclear p53 polyubiquitination, possibly via physiological depletion of nuclear DBC1, and that CBP and DBC1 play opposing roles in the genotoxic apoptotic pathway in cell lines retaining wild-type p53.

Restoration of DBC1 after Genotoxin Treatment Promotes Apoptosis

Because knockdown of DBC1 had only a minor effect on genotoxin-induced apoptosis due to the physiological loss of full-length DBC1 after genotoxin treatment (Figures 6B and 6C), we examined the effect of restoring full-length DBC1 levels in the setting of genotoxin treatment to better understand the role of DBC1 in genotoxin-induced apoptosis in the setting of wild-type (WT) p53. MCF-10A (immortalized non-transformed human breast ductal cell line), MCF-7, and U2OS cells, all with WT p53 function, were transiently transfected with control empty vector or DBC1 expression plasmid, treated with cisplatin, and either stained with apoptotic-dead cell markers annexin V-propidium iodide (PI) followed by flow cytometry or cell lysates immunoblotted for apoptotic markers, pro-apoptotic factors, and p53 (Figures 7A–7H). In addition, genotoxin-treated myc-DBC1-transfected U2OS cells were fractionated to check DBC1 overexpression in the nucleus and cytoplasm relative to physiological levels without stress, and rescue transfection restored DBC1 levels to near physiological (modestly increased) levels, especially in the nucleus, where DBC1’s effect on p53 stability is paramount (Figure S6B).

Overexpression of DBC1 in all three cell lines led to significantly increased (as much as doubling) early and late apoptotic events when compared with the control cells (Figures 7A–7F), suggesting that DBC1 regulates the apoptotic pathway in both normal and cancer cells. Similar results were obtained by immunoblotting, in which we observed increased cleaved PARP and cleaved caspase-3 and/or cleaved caspase-7 in cells overexpressing DBC1 when compared with vector-transfected control cells in all three cell lines treated with cisplatin (Figures 7G and 7H). In addition, we observed robust increases in the expression of BAX and PUMA, two pro-apoptotic factors regulated by p53, in cells overexpressing DBC1 in all three cell lines, compared with vector-transfected cisplatin-treated cells (Figures 7G and 7H).

Author Manuscript Author Manuscript Author Manuscript Author Manuscript

As a control to determine whether the effect of DBC1 overexpression on apoptosis is p53 dependent, U2OS cells transfected with control or DBC1 expression plasmids were treated with control or p53 siRNA (knockdown confirmed in Figure 7I), and cells were exposed to cisplatin as in Figure 7G. In contrast to results in control siRNA-treated cells, which mirrored those in Figure 7G, p53 depletion by siRNA abrogated apoptotic induction, because no cleaved caspase-3 and barely detectable cleaved PARP were observed, along with blunted BAX and PUMA induction (Figure 7I). Thus, DBC1 promotes apoptosis in cisplatin-treated cells specifically requiring p53, and stress-related cleavage or depletion of DBC1 appears to be a physiological counter-regulatory mechanism that attenuates at least cisplatin and possibly other genotoxin and stress-related apoptosis.

DISCUSSION

CBP and p300 are double-edged regulators of p53, contributing to both p53 degradation and stability. Under physiological cell conditions, the N-terminal regions of cytoplasmic, but not nuclear, CBP and p300 encode E3 and E4 ubiquitin ligase activities that, in conjunction with MDM2, destabilize p53 (Grossman et al., 2003; Shi et al., 2009; Ferreon et al., 2009). However, the compartment-specific regulation of the ubiquitin ligase activities of CBP is not understood. In this work, we found that DBC1, which is known to negatively regulate the activities of the deacetylases SIRT1 and HDAC3 (Zhao et al., 2008; Chini et al., 2010) and the epigenetic modifier SUV3H1 (Li et al., 2009), stably interacts with CBP in the nucleus and cytoplasm and strongly inhibits nuclear CBP E3-E4 ubiquitin ligase activities.

Although DBC1 was initially identified as being deleted from certain breast cancers, its function in human cancer is controversial, because it can either promote or suppress tumorigenesis (Hamaguchi et al., 2002; Kim et al., 2009; Zhang et al., 2014; Cha et al., 2009; Zhao et al., 2008; Won et al., 2015). In addition, DBC1 plays roles in the negative regulation of the nuclear receptor estrogen receptor (ER) (Koyama et al., 2010) and in the positive regulation of nuclear receptors such as AR, Rev-erb, and ER (Fu et al., 2009; Chini et al., 2013; Trauernicht et al., 2007).

We mapped DBC1/CBP interaction domains to the N terminus of DBC1, which interacts with both N- and C-terminal regions of CBP (Figures 3B and 3C). The N- and C-terminal regions of CBP are essential regulators of p53 stability and transactivation (Lill et al., 1997; Grossman, 2001). The N terminus of CBP promotes p53 degradation, while the C terminus of CBP is necessary for p53 stabilization and transactivation (Lill et al., 1997; Grossman, 2001). Because otherwise inactive nuclear CBP autoubiquitination activity was activated by DBC1 silencing, binding of the DBC1 N terminus to CBP deactivates nuclear CBP E3 ubiquitin ligase function, which forms the enzymatic core of CBP's E4 function (Shi et al., 2009). We have thus characterized the N-terminal region of DBC1 as a suppressor of CBP E3 ubiquitin ligase activity.

The amino acid sequences that are required for CBP E3 ubiquitin ligase activity also encode CBP E4 polyubiquitin ligase function for polyubiquitination of p53, which in co-operation with the E3 (mono)ubiquitin ligase activity of MDM2, maintains physiological p53 levels (Brooks et al., 2004; Grossman et al., 2003; Shi et al., 2009; Ferreon et al., 2009). We found

Author Manuscript Author Manuscript Author Manuscript Author Manuscript

that p53 is destabilized in DBC1-depleted cells (Figures 4 and 5), similar to findings in a prior report in which DBC1 suppressed tumorigenesis in a mouse model by regulating p53 stability (Qin et al., 2015). Although that work suggested that DBC1 regulates p53 by interrupting MDM2-p53 interaction, we found that in human cells, DBC1 binds to and inhibits CBP E4 polyubiquitination function toward p53, and the effect of DBC1 depletion on (increasing) p53 polyubiquitination and (decreasing) stability was entirely reversed by CBP depletion (Figure 4). In addition, overexpression of the DBC1 N terminus (CBP interacting), but not the DBC1 C terminus (non-CBP interacting), was sufficient to reverse the increase in p53 polyubiquitination after DBC1 depletion (Figure 5), suggesting that DBC1 is a specific inhibitor of CBP ubiquitin ligase activities, especially toward p53, in the absence of cellular stress. DBC1 therefore regulates both MDM2-p53 binding in a mouse model and CBP-dependent p53 polyubiquitination in human cells. Further study is needed to clarify whether CBP E4 inhibition is also at play in DBC1 activity in mouse cells and whether MD2/p53 interaction is regulated by DBC1 in human cells, such that both mechanisms may operate simultaneously in regulation of p53.

Adding complexity to the understanding of DBC1 regulation of p53, DBC1 reportedly negatively regulates SIRT1 deacetylation of p53 (Zhao et al., 2008), which could in some contexts lead to hyperacetylation and stabilization (by blocking ubiquitination) of p53. However, depletion of SIRT1 did not rescue p53 loss in *Dbc1*$^{-/-}$ cells, and spontaneous tumor development in *Dbc1*$^{-/-}$ mice was independent of SIRT1 (Qin et al., 2015), suggesting that DBC1 stabilizes p53 and inhibits tumorigenesis in a SIRT1-independent manner.

Surprisingly for a p53 activator, DBC1 levels dropped sharply after treatment with various stress agents. DBC1 mRNA levels decreased in response to genotoxic and non-genotoxic insults (Figure 6D). In addition, caspase-dependent cleavage of the DBC1 amino terminal region (containing the nuclear localization signal [NLS]) has been observed after tumor necrosis factor alpha (TNF-α) treatment (Sundararajan et al., 2005), though it is unclear whether that mechanism may be operative in addition to the decrease in transcription observed after treatment with the agents employed in this work. The decrease in nuclear DBC1 protein levels after stress explains the sharp decrease in nuclear CBP-DBC1 interaction we observed in response to DNA damage (Figure 6C). This decrease in CBP-DBC1 complex formation (without an accompanying drop in CBP protein levels) thus explains the activation of nuclear CBP E3 autoubiquitination in response to DNA damage (Figure S5), which is of a similar scale as observed that after DBC1 knockdown (Figure 3D). This DNA damage-induced activation of nuclear CBP ubiquitin ligase activity also explains the increase in nuclear p53 polyubiquitination in response to genotoxic stress (Figures 6A and S4A). We therefore propose that activation of nuclear CBP ubiquitin ligase activity (as a result of stress-induced DBC1 loss) in response to DNA damage may act in post-repair clearance of stabilized p53, which would physiologically limit apoptotic outcomes in cells destined to survive after repair.

Consistent with this idea, forced maintenance of full-length DBC1 expression during genotoxic insult, when DBC1 mRNA and protein levels decrease (Figure 6D), led to an elevated apoptotic response to cisplatin (Figures 7A–7C), presumably through DBC1-

Author Manuscript Author Manuscript Author Manuscript Author Manuscript

mediated attenuation of the normal DNA damage-dependent activation of nuclear CBP E3-E4 activity toward p53 (Figure S5). Although several conflicting reports exist about the role of DBC1 in apoptosis as being either pro-apoptotic (Park et al., 2014; Zhao et al., 2008; Won et al., 2015; Zannini et al., 2012; Sundararajan et al., 2005) or anti-apoptotic (Hiraike et al., 2010; Park et al., 2013), our results support DBC1 augmentation of p53-dependent apoptosis, and cells have clearly developed mechanisms to finely tune the abundance of DBC1 after stress to avoid exaggerated apoptotic responses.

Overall, this work has shed light on the role of DBC1 in the complex CBP/p53 pathway. We have solved a long-standing mystery of why CBP E3-E4 activity is only detected in the cytoplasm, and not in the nucleus, with implications for understanding the true function of nuclear CBP E3-E4 activities actively regulated by DBC1. TCGA data demonstrate preferential retention of WT p53 in DBC1-deleted tumors (Figure 2), suggesting DBC1 loss is another means of tumorigenic p53 pathway disruption. Our findings open avenues for strategic restoration of DBC1 function to reactivate p53 tumor-suppressive activities in tumors with DBC1 alterations and WT p53 status. Such approaches could, for example, lead to therapies that restore platinum sensitivity in platinum-resistant tumors retaining WT p53, such as in breast and lung cancers (Horton, 1995; Luvero et al., 2014; Wang et al., 2016; Eckstein, 2011; Sarin et al., 2017), or lead to therapeutic approaches in prostate cancer, in which DBC1 loss occurs at the highest frequency of any human cancer.

STAR★METHODS

CONTACT FOR REAGENT AND RESOURCE SHARING

Further information and requests for reagents may be directed to, and will be fulfilled by the corresponding author, Steven Grossman (steven.grossman@vcuhealth.org).

EXPERIMENTAL MODEL AND SUBJECT DETAILS

Cell lines

U2OS and MCF7 cells: U2OS cells (human osteosarcoma cells; female; ATCC) and MCF7 cells (epithelial breast cancer cells; female; the generous gift of J. Koblinski) were cultured and maintained in DMEM (High glucose, L-glutamine, Pyruvate) with 10% fetal bovine serum and 100μL/mL penicillin at 37°C incubator with 5% CO_2.

HEK293T cells: HEK293T cells (human embryonic kidney cells transformed by SV40 large T antigen; female; ATCC) were cultured and maintained in DMEM (High glucose, L-glutamine, Pyruvate) with 10% fetal bovine serum and 100μL/mL penicillin at 37°C incubator with 5% CO_2.

H1299 cells: H1299 cells (human lung carcinoma cells; male; ATCC) were cultured and maintained in RPMI with 10% fetal bovine serum and 100μL/mL penicillin at 37°C incubator with 5% CO_2.

MCF10-A cells: MCF10-A cells (epithelial breast cells; female; the generous gift of J. Koblinski) were cultured and maintained in DMEM/F12 with 5% horse serum, 20ng/mL

Author Manuscript Author Manuscript Author Manuscript Author Manuscript

EGF, 0.5mg/mL hydrocortisone, 100ng/mL cholera toxin, 10μg/mL insulin and 10% penicillin at 37°C incubator with 5% CO_2.

METHOD DETAILS

Induction of DNA Damage—Cells were grown to 80% confluency before treatment with either cisplatin (Selleckchem, Houston, TX), staurosporine (Cell Signaling, Beverly, MA), doxorubicin (Sigma-Aldrich), or etoposide (Sigma-Aldrich) where indicated.

Subcellular Fractionation—Cytoplasmic and nuclear extracts of U2OS and H1299 cells were prepared using the NE-PER Nuclear and Cytoplasmic Extraction kit purchased from Thermo-Fisher Scientific (Waltham, MA).

In-Vitro E3 Assays of CBP—To determine CBP E3 ligase activity, CBP was immunoprecipitated from cytoplasm or nuclear fractions diluted with high salt buffer [10mMHEPES(pH7.5), 150mM NaCl, 150mMKCl, 1mMMgCl2, 0.5%Triton X-100, supplemented with protease inhibitors), using A-22 antibody and protein A Sepharose. The IPs were washed in high salt buffer three times followed by two washes in Ub buffer (25mMHEPES, pH7.4,10mMNaCl, 3 mM MgCl2, 0.05% Triton X-100, 0.5 mM DTT, 3 mM Mg-ATP). The washed and equilibrated IPs were then incubated with 100 ng E1 (rabbit; Boston Biochem), 25ng E2 (UbcH5a, human recombinant; Boston Biochem), and 5μg Ub (human recombinant; Boston Biochem) for 60 min at 37°C. Reactions were then stopped by the addition of LDS sample buffer, followed by SDS-PAGE and immunoblotting.

MudPIT Analysis—U2OS cells were fractionated into cytoplasmic and nuclear fractions followed by CBP IP from both fractions using anti CBP conjugated agarose beads. Eluates were separated by SDS-PAGE followed by Coomassie staining. Mass spectrometry analysis was carried out at the proteomics core of the University of Virginia (UVA). Briefly, the gel piece was transferred to a siliconized tube and washed and destained in 200μL 50% methanol for 3hours. The gel pieces were dehydrated in acetonitrile, rehydrated in 30μL of 10mM dithiolthreitol in 0.1M ammonium bicarbonate and reduced at room temperature. After 2 steps of dehydrating the gel pieces in acetonitrile and rehydrating in ammonium bicarbonate, samples were digested overnight at 37°C followed by peptide extraction and MS analysis. The LC-MS system consisted of a Thermo Electron Orbitrap Velos ETD mass spectrometer system with a Protana nanospray ion source. The digest was analyzed using the rapid switching capability of the instrument acquiring full scan mass spectra to determine peptide molecular weights followed by product ion spectra to determine amino acid sequence in sequential scans. The data were analyzed by database searching using the Sequest search algorithm against IPI Human.

Western Blotting, IP and Immunofluorescence—For western blot analyses, cytoplasmic and nuclear extracts of cells were prepared using NE-PER fractionation kit followed by SDS-PAGE and immunoblotting. For whole cell lysates, cells were lysed in RIPA buffer. For IPs, cytoplasmic and nuclear extracts were diluted with NP40 lysis buffer [25mM Tris HCl (pH 7.5), 150mM NaCl, 1μM $ZnCl_2$, 1% igepal (NP40)], supplemented with protease inhibitors, and incubated overnight at 4°C with the indicated antibodies and

Author Manuscript Author Manuscript Author Manuscript Author Manuscript

either Protein A agarose (for antibodies raised in rabbit) or Protein G agarose (for antibodies raised in mouse). IP eluates were subjected to SDS-PAGE and immunoblotting following three washes in IP lysis buffer. For immunofluorescence, cells were fixed in 4% paraformaldehyde, washed with PBS and permeabilized with 0.2% Triton X-100 in PBS for 10 minutes. Cells were blocked in Odyssey blocking buffer (Li-Cor, 927-4000) for 1 hour at room temperature followed by overnight incubation at 4°C in primary antibody. After washing with PBS, cells were incubated for 1 hour at room temperature in the dark in secondary antibodies. At last, cells were counterstained with DAPI (Thermo-Fisher). Images were acquired using an EVOS AMG (Thermo-Fisher) fluorescent microscope and representative images are shown at the same exposure and magnification.

Generation of Knockdown Cell Lines—DBC1 and CBP single or double knockdown stable cell lines were made in the U2OS parent line using Mission shRNA lentiviral vector from Sigma-Aldrich (St. Louis, MO) and GIPZ lentiviral shRNA vector from GE Healthcare Dharmacon (Lafayette, Colorado), respectively. DBC1 Mission shRNA clone IDs are: NM_021174.4-1597s1c1 and NM_021174.4-1125s1c1.

GIPZ CREBBP shRNAs tested for knockdown level are: V2LHS_24251, V3LHS_358933, V3LHS_358934, and V3LHS_358935. Lentiviruses were produced in HEK293T cells by calcium phosphate mediated transfection using pLKO.1-shRNA or pGIPZ-shRNA plasmids. U2OS cells were transduced with virus medium and DMEM containing 5μg/ml puromycin was used to select the DBC1sh and CBPsh cells 48 hours post-infection. DBC1sh cells were subsequently used to make the DBC1/CBP double knockdown line.

siRNA Transfection—CBP siRNA was purchased from Ambion (Foster City, CA). DBC1 SMARTpool ON-TARGET plus siRNA and p53 SMARTpool ON-TARGET plus siRNA were purchased from Dharmacon. U2OS cells were transfected with siRNA (30nM final concentration) using Lipofectamine 2000 (Thermo-Fisher Scientific). Cells were harvested 72 hours post transfection.

Plasmids and Expression of Recombinant proteins—Full length FLAG-CBP and truncated mutants of CBP were previously described (Shi et al., 2009). DBC1 was divided into three different regions, DBC1 (1-240aa), DBC1 (1-470aa) and DBC1 (697-923aa) based on its globular domain structure. Plasmids for overexpressing these truncated DBC1 proteins in mammalian cells were constructed by amplifying DBC1 from the parent plasmid, a myc-tagged full length DBC1 expression vector, from Addgene (#35096, Cambridge, MA). Amplified fragments were cloned back into the original expression vector (pcDNA3.0) used for expressing full length DBC1. Primers used are listed in Table S1.

Generation of shRNA resistant plasmids—shRNA resistant myc-DBC1* and myc-DBC1(1-470)* plasmids were constructed by generating silent mutations in the region targeted by Sigma siRNA of the DBC1 ORF. The silent mutations were generated by Gene Splicing by Overlap Extension (Gene SOEing) method, as previously in Horton (1995). The final DNA fragment was digested with EcoRI and *XhoI* endonucleases and ligated to the linearized myc-tagged vector. Flanking and SOEing primers used are listed in Table S1.

Author Manuscript Author Manuscript Author Manuscript Author Manuscript

Isolation of RNA and RT-PCR—RNA was isolated from U2OS cells using the RNeasy Plus Mini Kit (QIAGEN, Hilden, Germany). cDNA was prepared using the SensiFAST™ cDNA Synthesis Kit (London, UK) followed by quantitative Real-Time PCR using SYBR Green (Applied Biosystems, Foster City, CA). Relative quantitation was carried out using the comparative C_T Method ($\Delta\Delta C_T$ Method). RT-PCR primers are listed in Table S1.

Apoptosis assay by Flow cytometry—Apoptosis assessment was made based on APC Annexin V and PI staining. Cells were treated with 25 μM cisplatin for 24hrs followed by staining with APC Annexin V and PI as described in Life Technologies (Thermo Fisher) Apoptosis Assay protocol. Cells were analyzed by flow cytometry using a BD (Franklin Lakes, NJ) FACS Canto II.

Active Caspase 3 assay by Flow cytometry: Cisplatin treated cells were fixed and permeabilized using Cytofix/Cytoperm Fixation/Permeabilization kit (BD Biosciences, San Diego, CA) followed by staining with Alexa Fluor 647 Rabbit Anti-Active Caspase 3 antibody (BD Biosciences). Stained cells were analyzed by flow cytometry for active caspase 3 activity.

QUANTIFICATION AND STATISTICAL ANALYSIS

MudPIT Data Analysis—Data generated from MudPIT were processed using the Scaffold Proteome Software.

Statistical analysis: All statistical tests were carried out using Graph Pad Prism version 5.0 for Windows (Graph Pad Software, San Diego, CA). N = 3 biological replicates for each condition examined. Statistical parameters including S.D, SEM and statistical significance are reported in the figures and supplementary figures.

DATA AND SOFTWARE AVAILABILITY

The mass spectrometry proteomics data have been deposited to the ProteomeXchange Consortium via the PRIDE [1] partner repository with the dataset identifier PRIDE: PXD012673.

Supplementary Material

Refer to Web version on PubMed Central for supplementary material.

ACKNOWLEDGMENTS

We thank J. Koblinski for generously providing the MCF-7 and MCF-10A cell lines. Services and products in support of the research project were generated by the VCU Massey Cancer Center Flow Cytometry Shared Resource, supported in part with funding from NIH-NCI Cancer Center support grant P30 CA016059. S.R.G. was supported by R01 CA107532 and P30 CA016059.

REFERENCES

Arany Z, Huang LE, Eckner R, Bhattacharya S, Jiang C, Goldberg MA, Bunn HF,and Livingston DM(1996).An essential role for p300/CBP in the cellular response to hypoxia. Proc. Natl. Acad. Sci. USA 93, 12969–12973. [PubMed: 8917528]

Author Manuscript Author Manuscript Author Manuscript Author Manuscript

Bannister AJ, and Kouzarides T (1996). The CBP co-activator is a histone acetyltransferase. Nature 384, 641–643. [PubMed: 8967953]

Bode AM, and Dong Z (2004). Post-translational modification of p53 in tumorigenesis. Nat. Rev. Cancer 4, 793–805. [PubMed: 15510160]

Brooks CL, and Gu W (2003). Ubiquitination, phosphorylation and acetylation: the molecular basis for p53 regulation. Curr. Opin. Cell Biol 15,164–171. [PubMed: 12648672]

Brooks CL, Li M, and Gu W (2004). Monoubiquitination: the signal for p53 nuclear export? Cell Cycle 3, 436–438. [PubMed: 14976431]

Cerami E, Gao J, Dogrusoz U, Gross BE, Sumer SO, Aksoy BA, Jacobsen A, Byrne CJ, Heuer ML, Larsson E, et al. (2012). The cBio cancer genomics portal: an open platform for exploring multidimensional cancer genomics data. Cancer Discov. 2, 401–404. [PubMed: 22588877]

Cha EJ, Noh SJ, Kwon KS, Kim CY, Park BH, Park HS, Lee H, Chung M, Kang MJ, Lee DG, et al. (2009). Expression of DBC1 and SIRT1 is associated with poor prognosis of gastric carcinoma. Clin. Cancer Res 15, 4453–4459. [PubMed: 19509139]

Chan HM, and La Thangue NB (2001). p300/CBP proteins: HATs for transcriptional bridges and scaffolds. J. Cell Sci 114, 2363–2373. [PubMed: 11559745]

Chini CC, Escande C, Nin V, and Chini EN (2010). HDAC3 is negatively regulated by the nuclear protein DBC1. J. Biol. Chem 285, 40830–40837. [PubMed: 21030595]

Chini CC, Escande C, Nin V, and Chini EN (2013). DBC1 (Deleted in Breast Cancer 1) modulates the stability and function of the nuclear receptor Rev-erbα. Biochem. J. 451, 453–461. [PubMed: 23398316]

Chrivia JC, Kwok RP, Lamb N, Hagiwara M, Montminy MR, and Goodman RH (1993). Phosphorylated CREB binds specifically to the nuclear protein CBP. Nature 365, 855–859. [PubMed: 8413673]

Dietze EC, Bowie ML, Mrózek K, Caldwell LE, Neal C, Marjoram RJ, Troch MM, Bean GR, Yokoyama KK, Ibarra CA, and Seewaldt VL (2005). CREB-binding protein regulates apoptosis and growth of HMECs grown in reconstituted ECM via laminin-5. J. Cell Sci 118, 5005–5022. [PubMed: 16219677]

Eckstein N (2011). Platinum resistance in breast and ovarian cancer cell lines. J. Exp. Clin. Cancer Res 30, 91. [PubMed: 21967738]

Ferreon JC, Lee CW, Arai M, Martinez-Yamout MA, Dyson HJ, and Wright PE (2009). Cooperative regulation of p53 by modulation of ternary complex formation with CBP/p300 and HDM2. Proc. Natl. Acad. Sci. USA 106, 6591–6596. [PubMed: 19357310]

Fu J, Jiang J, Li J, Wang S, Shi G, Feng Q, White E, Qin J, and Wong J (2009). Deleted in breast cancer 1, a novel androgen receptor (AR) coactivator that promotes AR DNA-binding activity. J. Biol. Chem 284, 6832–6840. [PubMed: 19126541]

Gao J, Aksoy BA, Dogrusoz U, Dresdner G, Gross B, Sumer SO, Sun Y, Jacobsen A, Sinha R, Larsson E, et al. (2013). Integrative analysis of complex cancer genomics and clinical profiles using the cBioPortal. Sci. Signal 6, pl1. [PubMed: 23550210]

Goodman RH, and Smolik S (2000). CBP/p300 in cell growth, transformation, and development. Genes Dev. 14, 1553–1577. [PubMed: 10887150]

Grossman SR (2001). p300/CBP/p53 interaction and regulation of the p53 response. Eur. J. Biochem 268, 2773–2778. [PubMed: 11358491]

Grossman SR, Deato ME, Brignone C, Chan HM, Kung AL, Tagami H, Nakatani Y, and Livingston DM (2003). Polyubiquitination of p53 by a ubiquitin ligase activity of p300. Science 300, 342–344. [PubMed: 12690203]

Hamaguchi M, Meth JL, von Klitzing C, Wei W, Esposito D, Rodgers L, Walsh T, Welcsh P, King MC, and Wigler MH (2002). DBC2, a candidate for a tumor suppressor gene involved in breast cancer. Proc. Natl. Acad. Sci. USA 99, 13647–13652. [PubMed: 12370419]

Hiraike H, Wada-Hiraike O, Nakagawa S, Koyama S, Miyamoto Y, Sone K, Tanikawa M, Tsuruga T, Nagasaka K, Matsumoto Y, et al. (2010). Identification of DBC1 as a transcriptional repressor for BRCA1. British J. Cancer 102, 1061–1067.

Horton RM (1995). PCR-mediated recombination and mutagenesis. SOEing together tailor-made genes. Mol. Biotechnol 3, 93–99. [PubMed: 7620981]

Author Manuscript Author Manuscript Author Manuscript Author Manuscript

Kaur M, Pop M, Shi D, Brignone C, and Grossman SR (2007). hHR23B is required for genotoxic-specific activation of p53 and apoptosis. Oncogene 26, 1231–1237. [PubMed: 16924240]

Kim JE, Chen J, and Lou Z (2009). p30 DBC is a potential regulator of tumorigenesis. Cell Cycle 8, 2932–2935. [PubMed: 19657230]

Koegl M, Hoppe T, Schlenker S, Ulrich HD, Mayer TU, and Jentsch S (1999). A novel ubiquitination factor, E4, is involved in multiubiquitin chain assembly. Cell 96, 635–644. [PubMed: 10089879]

Koyama S, Wada-Hiraike O, Nakagawa S, Tanikawa M, Hiraike H, Miyamoto Y, Sone K, Oda K, Fukuhara H, Nakagawa K, et al. (2010). Repression of estrogen receptor beta function by putative tumor suppressor DBC1. Biochem. Biophys. Res. Commun. 392, 357–362. [PubMed: 20074560]

Li M, Brooks CL, Wu-Baer F, Chen D, Baer R, and Gu W (2003). Mono-versus polyubiquitination: differential control of p53 fate by Mdm2. Science 302, 1972–1975. [PubMed: 14671306]

Li Z, Chen L, Kabra N, Wang C, Fang J, and Chen J (2009). Inhibition of SUV39H1 methyltransferase activity by DBC1. J. Biol. Chem. 284, 10361–10366. [PubMed: 19218236]

Lill NL, Grossman SR, Ginsberg D, DeCaprio J, and Livingston DM (1997). Binding and modulation of p53 by p300/CBP coactivators. Nature 387, 823–827. [PubMed: 9194565]

Luvero D, Milani A, and Ledermann JA (2014). Treatment options in recurrent ovarian cancer: latest evidence and clinical potential. Ther. Adv. Med. Oncol 6, 229–239. [PubMed: 25342990]

Martinez-Balbás MA, Bannister AJ, Martin K, Haus-Seuffert P, Meisterernst M, and Kouzarides T (1998). The acetyltransferase activity of CBP stimulates transcription. EMBO J. 17, 2886–2893. [PubMed: 9582282]

Ogryzko VV, Schiltz RL, Russanova V, Howard BH, and Nakatani Y (1996). The transcriptional coactivators p300 and CBP are histone acetyltransferases. Cell 87, 953–959. [PubMed: 8945521]

Park JH, Lee SW, Yang SW, Yoo HM, Park JM, Seong MW, Ka SH, Oh KH, Jeon YJ, and Chung CH (2014). Modification of DBC1 by SUMO2/3 is crucial for p53-mediated apoptosis in response to DNA damage. Nat. Commun. 5, 5483. [PubMed: 25406032]

Park SH, Riley P 4th, and Frisch SM (2013). Regulation of anoikis by deleted in breast cancer-1 (DBC1) through NF-κB. Apoptosis 18, 949–962. [PubMed: 23588592]

Qin B, Minter-Dykhouse K, Yu J, Zhang J, Liu T, Zhang H, Lee S, Kim J, Wang L, and Lou Z (2015). DBC1 functions as a tumor suppressor by regulating p53 stability. Cell Rep. 10, 1324–1334. [PubMed: 25732823]

Saito S, Yamaguchi H, Higashimoto Y, Chao C, Xu Y Jr., Fornace AJ Jr., Appella E, and Anderson CW (2003). Phosphorylation site interdependence of human p53 post-translational modifications in response to stress. J. Biol. Chem 278, 37536–37544. [PubMed: 12860987]

Sarin N, Engel F, Kalayda GV, Mannewitz M, Cinati J Jr., Rothweiler F, Michaelis M, Saafan H, Ritter CA, Jaehde U, and Frötschl R (2017). Cisplatin resistance in non-small cell lung cancer cells is associated with an abrogation of cisplatin-induced G2/M cell cycle arrest. PLoS One 12, e0181081. [PubMed: 28746345]

Shi D, Pop MS, Kulikov R, Love IM, Kung AL, and Grossman SR (2009). CBP and p300 are cytoplasmic E4 polyubiquitin ligases for p53. Proc. Natl. Acad. Sci. USA 106, 16275–16280. [PubMed: 19805293]

Sundararajan R, Chen G, Mukherjee C, and White E (2005). Caspase-dependent processing activates the proapoptotic activity of deleted in breast cancer-1 during tumor necrosis factor-alpha-mediated death signaling. Oncogene 24, 4908–4920. [PubMed: 15824730]

Symonds H, Krall L, Remington L, Saenz-Robles M, Lowe S, Jacks T, and Van Dyke T (1994). p53-dependent apoptosis suppresses tumor growth and progression in vivo. Cell 78, 703–711. [PubMed: 8069917]

Trauernicht AM, Kim SJ, Kim NH, and Boyer TG (2007). Modulation of estrogen receptor alpha protein level and survival function by DBC-1. Mol. Endocrinol 21, 1526–1536. [PubMed: 17473282]

Turnell AS, and Mymryk JS (2006). Roles for the coactivators CBP and p300 and the APC/C E3 ubiquitin ligase in E1A-dependent cell transformation. Br. J. Cancer 95, 555–560. [PubMed: 16880778]

Author Manuscript Author Manuscript Author Manuscript Author Manuscript

Turnell AS, Stewart GS, Grand RJ, Rookes SM, Martin A, Yamano H, Elledge SJ, and Gallimore PH (2005). The APC/C and CBP/p300 cooperate to regulate transcription and cell-cycle progression. Nature 438, 690–695. [PubMed: 16319895]

Vervoorts J, Lüscher-Firzlaff JM, Rottmann S, Lilischkis R, Walsemann G, Dohmann K, Austen M, and Lüscher B (2003). Stimulation of c-MYC transcriptional activity and acetylation by recruitment of the cofactor CBP. EMBO Rep. 4, 484–490. [PubMed: 12776737]

Wang Y, Krais JJ, Bernhardy AJ, Nicolas E, Cai KQ, Harrell MI, Kim HH, George E, Swisher EM, Simpkins F, and Johnson N (2016). RING domain-deficient BRCA1 promotes PARP inhibitor and platinum resistance. J. Clin. Invest 126, 3145–3157. [PubMed: 27454289]

Won KY, Cho H, Kim GY, Lim SJ, Bae GE, Lim JU, Sung JY, Park YK, Kim YW, and Lee J (2015). High DBC1 (CCAR2) expression in gallbladder carcinoma is associated with favorable clinicopathological factors. Int. J. Clin. Exp. Pathol 8, 11440–11445. [PubMed: 26617872]

Yates JR, Ruse CI, and Nakorchevsky A (2009). Proteomics by mass spectrometry: approaches, advances, and applications. Annu. Rev. Biomed. Eng 11, 49–79. [PubMed: 19400705]

Zannini L, Buscemi G, Kim JE, Fontanella E, and Delia D (2012). DBC1 phosphorylation by ATM/ATR inhibits SIRT1 deacetylase in response to DNA damage. J. Mol. Cell Biol 4, 294–303. [PubMed: 22735644]

Zhang Y, Gu Y, Sha S, Kong X, Zhu H, Xu B, Li Y, and Wu K (2014). DBC1 is over-expressed and associated with poor prognosis in colorectal cancer. Int. J. Clin. Oncol 19, 106–112. [PubMed: 23299276]

Zhao W, Kruse JP, Tang Y, Jung SY, Qin J, and Gu W (2008). Negative regulation of the deacetylase SIRT1 by DBC1. Nature 451, 587–590. [PubMed: 18235502]

Author Manuscript Author Manuscript Author Manuscript Author Manuscript

Highlights

- DBC1 attenuates CBP's p53-directed ubiquitin ligase activity, stabilizing p53
- DBC1 loss is positively correlated with retention of wild-type p53 in solid tumors
- Decrease in nuclear DBC1 with stress limits the p53-dependent apoptotic response
- Restoration of nuclear DBC1 with genotoxic stress promotes p53-dependent apoptosis

Author Manuscript Author Manuscript Author Manuscript Author Manuscript

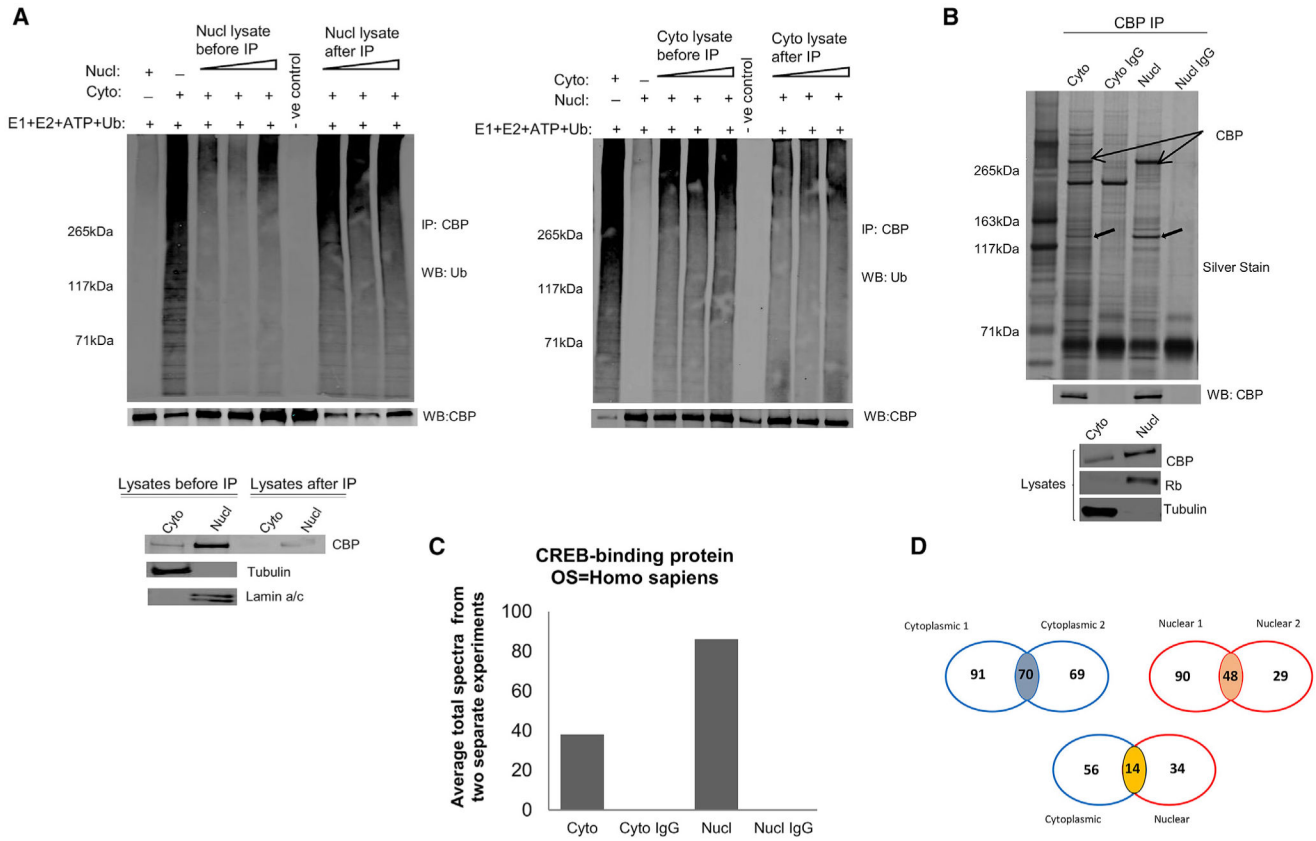

Figure 1. Identification of CBP-Interacting Proteins in U2OS Cells

(A) Identification of activators and/or inhibitors of CBP E3 activity. (Left) CBP IP from nuclear fractions (lane 1) or cytoplasmic fractions (lanes 2–9), followed by incubation of cytoplasmic CBP IPs with either nuclear lysate (lanes 3–5) or nuclear lysate after CBP immunodepletion (lanes 7–9), followed by *in vitro* CBP E3 autoubiquitination assay (addition of ubiquitin reaction components ATP, ubiquitin (Ub), E1, and E2 to the washed IP; lanes 1–5 and 7–9) or mock assay (no reaction components, buffer only; lane 6) and immunoblotting of the reaction products with the indicated antibodies. (Right) CBP IP from cytoplasmic fractions (lane 1) or nuclear fractions (lanes 2–9), followed by incubation of nuclear CBP IPs with either cytoplasmic lysate (lanes 3–5) or cytoplasmic lysate after CBP immunodepletion (lanes 7–9), followed by *in vitro* CBP E3 autoubiquitination assay and immunoblotting of the reaction products with the indicated antibodies. See also Figure S1.

(B) CBP IP from cytoplasmic and nuclear fractions of U2OS cells, followed by silver staining (top) or CBP immunoblotting (middle). (Bottom) Immunoblot of cytoplasmic and nuclear fractions for CBP and nuclear (Rb) and cytoplasmic (tubulin) specific markers.

(C) Graphical representation of the average total spectra of CBP identified by MudPIT analyses from cytoplasmic and nuclear CBP immunoprecipitations from two separate experiments.

(D) Venn diagrams of the number of overlapping and non-overlapping CBP-interacting proteins from cytoplasmic and nuclear CBP IPs identified by MudPIT from two separate experiments (upper) and common to both experiments (lower).

Author Manuscript Author Manuscript Author Manuscript Author Manuscript

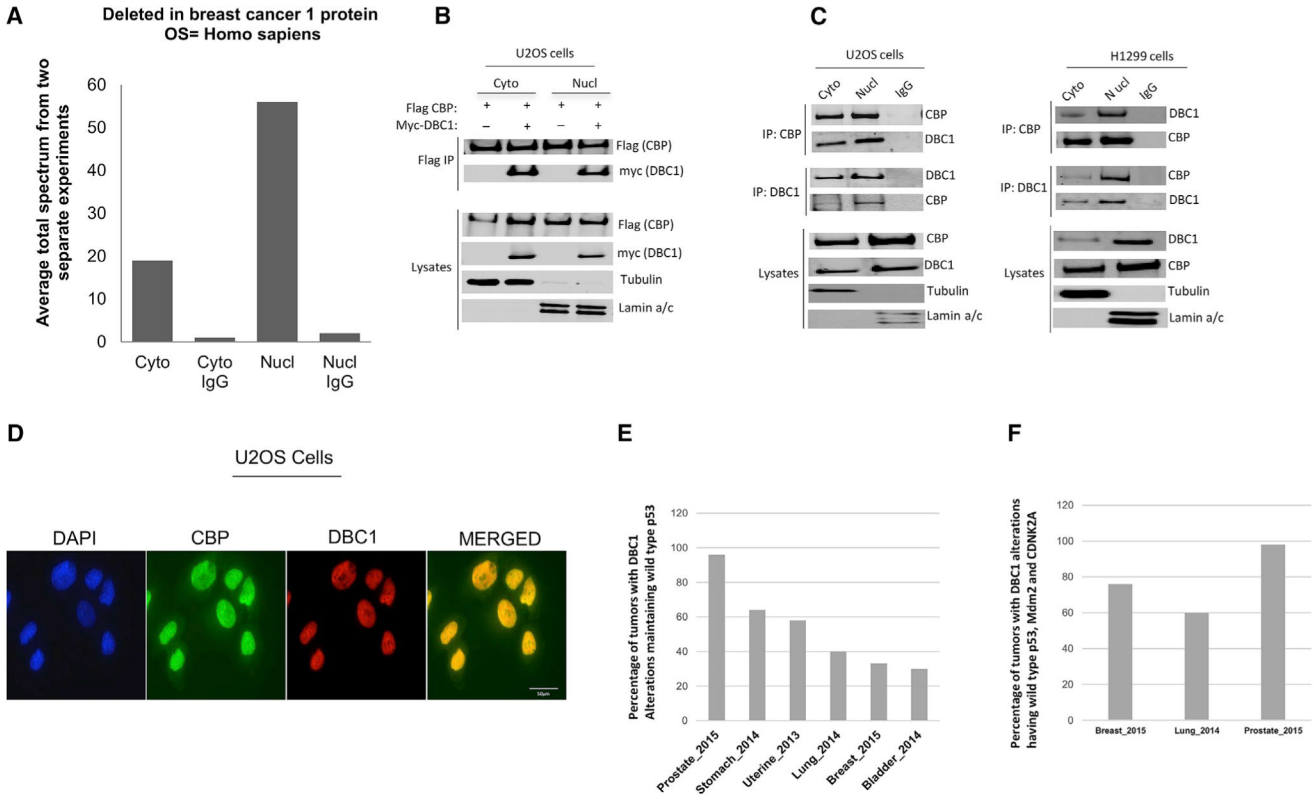

Figure 2. DBC1 Is a CBP-Interacting Protein

(A) Graphical representation of total spectra of DBC1 identified by MudPIT analysis from cytoplasmic and nuclear CBP IPs from two separate experiments.

(B) U2OS cells were transfected with FLAG-tagged CBP and myc-tagged DBC1 for 48 h, followed by FLAG IP (top) of nuclear and cytoplasmic lysates and immunoblotting of IPs using anti-FLAG and anti-myc antibodies. (Bottom) Immunoblotting of nuclear and cytoplasmic lysates used in each IP with indicated antibodies.

(C) CBP or DBC1 IPs (top) from cytoplasmic and nuclear fractions of U2OS cells (left) and H1299 cells (right), followed by immunoblotting. (Bottom) Immunoblots of nuclear and cytoplasmic lysates used in each IP.

(D) Immunofluorescent staining of U2OS cells using anti-CBP and anti-DBC1 antibodies. Images are representative of three independent experiments. See also Figure S2.

(E) Graphical representation of TCGA data showing the percentage of tumors with DBC1 alterations retaining wild-type p53.

(F) Graphical representation of TCGA data showing the percentage of human breast, lung, or prostate cancers with DBC1 loss retaining not only wild-type CBP and p53 but also wild-type status of the key p53 regulators MDM2 (non-amplified) and CDKN2A (not deleted).

Author Manuscript
Author Manuscript
Author Manuscript
Author Manuscript

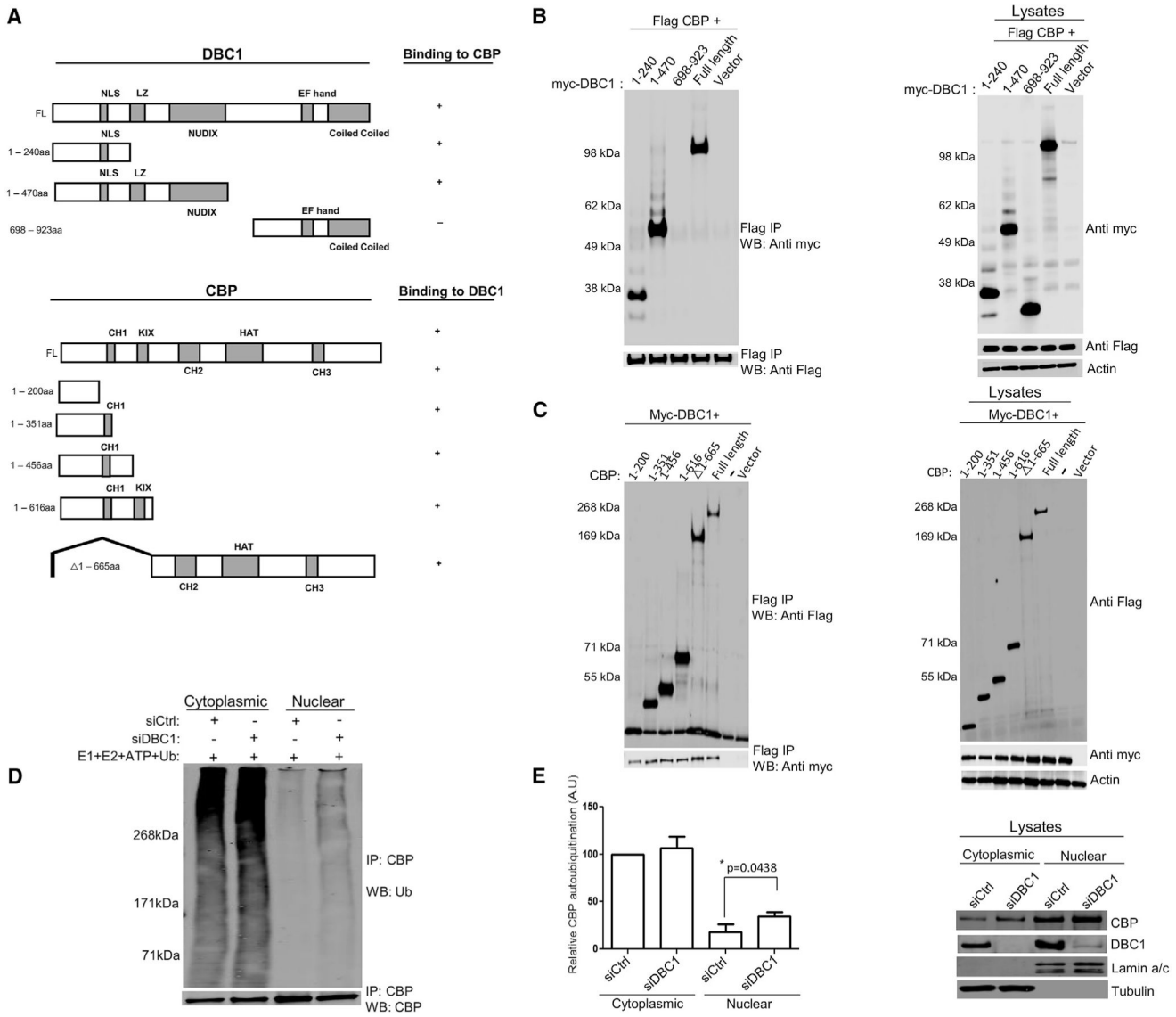

Figure 3. DBC1 Interacts with N- and C-Terminal Regions of CBP and Regulates Nuclear CBP E3 Ubiquitin Ligase Activity

(A) Schematic diagram of full-length DBC1, full-length CBP, and deletion mutants of DBC1 and CBP. NLS, nuclear localization signal; NES, nuclear export sequence; CH1, CH2, and CH3, cysteine-histidine regions.

(B and C) Plasmids encoding FLAG-tagged full-length CBP, along with myc-tagged full-length DBC1, DBC1 deletion constructs, or vector (B), or myc-tagged full-length DBC1, along with FLAG-tagged full-length CBP, CBP deletion constructs, or vector (C), were transfected into U2OS cells, followed by IPs with anti-FLAG antibody and immunoblotting with anti-FLAG and anti-myc antibodies. Right panels show immunoblotting of lysates.

(D) CBP IP from cytoplasmic and nuclear fractions of U2OS cells transfected with control or DBC1 siRNA, followed by *in vitro* CBP E3 autoubiquitination assay and immunoblotting of ubiquitination reactions.

(E) Quantification of CBP autoubiquitination in (D) by densitometry. Error bars represents mean ± SEM from three independent experiments. Right panel shows immunoblotting of lysates used for IPs in (D) with the indicated antibodies.

Author Manuscript Author Manuscript Author Manuscript Author Manuscript

Author Manuscript Author Manuscript Author Manuscript Author Manuscript

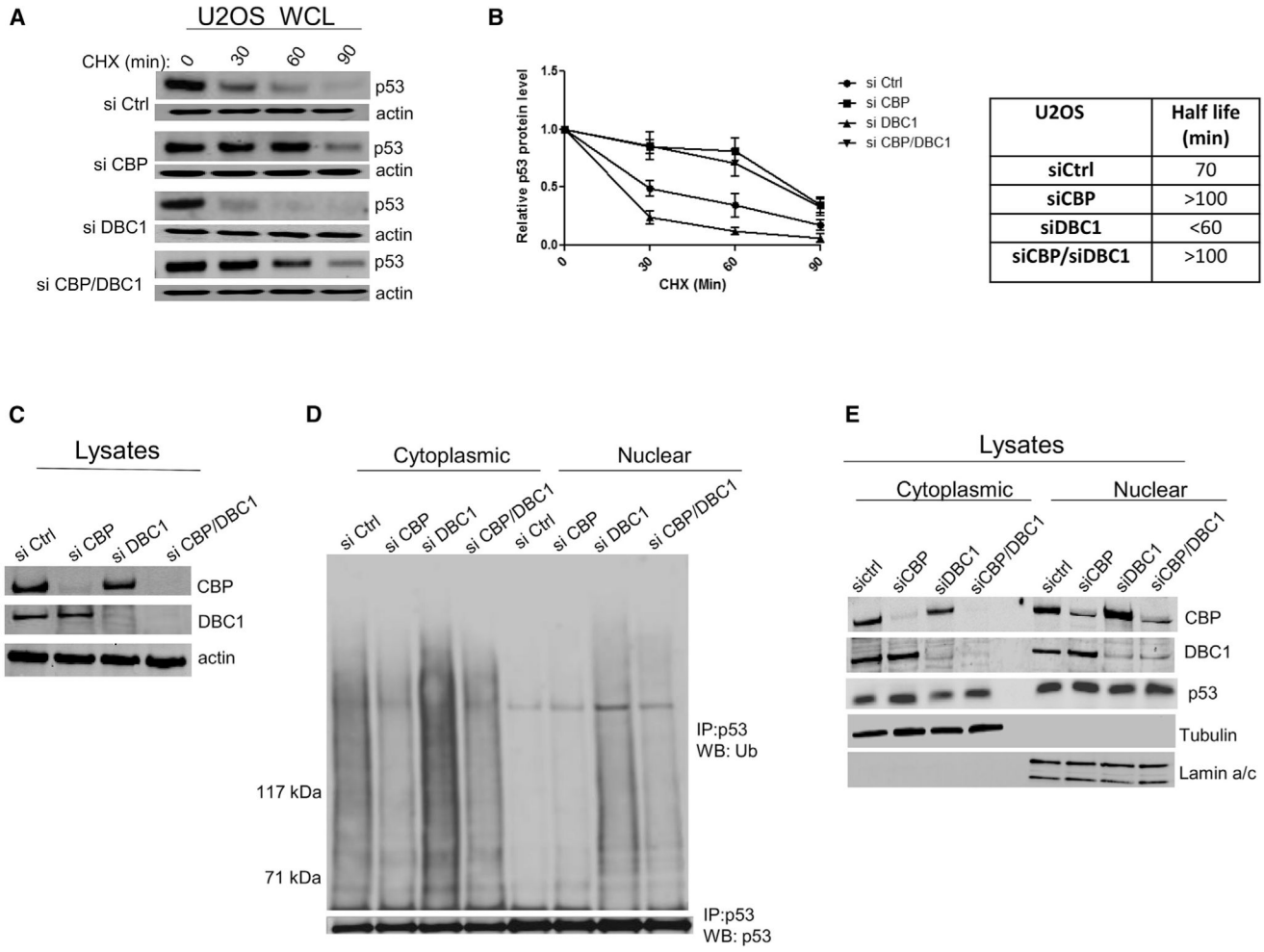

U2OS	Half life (min)
siCtrl	70
siCBP	>100
siDBC1	<60
siCBP/siDBC1	>100

Figure 4. DBC1 Depletion Decreases p53 Half-Life in U2OS Cells

(A) U2OS cells treated with 100 μM cycloheximide (Sigma) for up to 90 min were harvested for immunoblotting using anti-p53 antibody. See also Figure S3.

(B) Quantification of relative p53 protein level post-cycloheximide treatment. (Left) Error bars represent mean ± SD from three independent experiments. (Right) Derived p53 half-life is displayed in the table.

(C) Immunoblotting of lysates from (A).

(D) p53 IPs from cytoplasmic and nuclear fractions of U2OS cells treated with control, CBP, DBC1, or CBP-DBC1 siRNA, followed by immunoblotting with anti-p53 and ubiquitin antibodies.

(E) Immunoblotting of cytoplasmic and nuclear lysates from (D).

Author Manuscript Author Manuscript Author Manuscript Author Manuscript

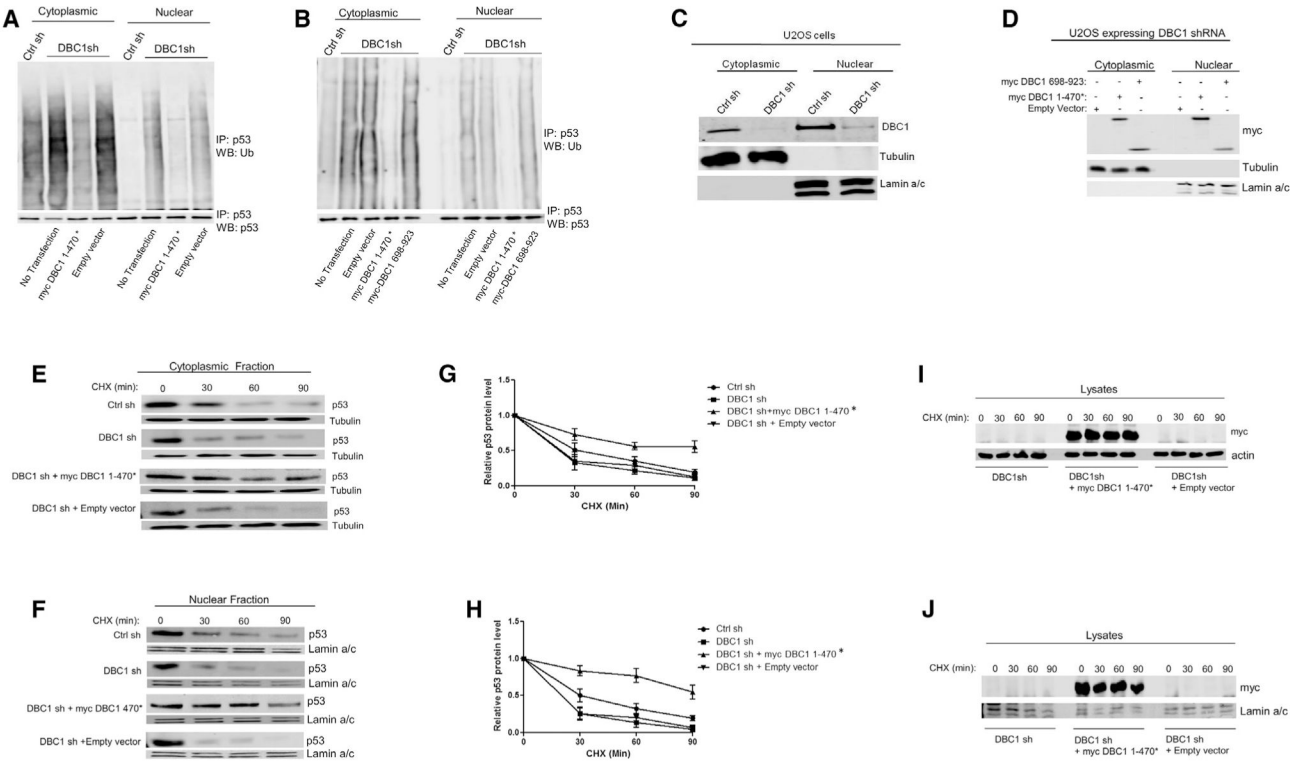

Figure 5. Re-expression of DBC1 Reduces p53 Polyubiquitination and Stabilizes p53 in DBC1-Depleted Cells

(A and B) p53 IPs from cytoplasmic and nuclear fractions of U2OS cells (A) stably expressing DBC1 shRNA transfected with either empty vector or DBC1(1–470)* or (B) transfected with constructs in (A) and DBC1(698–923), followed by immunoblotting. Cells expressing control shRNA were included in this experiment.

(C and D) Immunoblots of U2OS nuclear and cytoplasmic fractions used in (A) and (B), showing (C) DBC1 knockdown, (D) overexpression of DBC1(1–470)*, and overexpression of DBC1(698–923) in DBC1 shRNA-expressing cells.

(E and F) U2OS cells stably expressing DBC1 shRNA, transfected with either empty vector or DBC1(1–470)*, were treated with 100 μM cycloheximide for up to 90 min and harvested for subcellular fractionation, followed by immunoblotting of (E) cytoplasm and (F) nuclear fractions with p53, tubulin, and lamin a/c antibodies.

(G and H) Quantification of p53 half-life in the cytoplasmic (G) and nuclear (H) fractions from (E) and (F). Error bars represent mean ± SD from three independent experiments.

(I and J) Immunoblots of cytoplasmic (I) and nuclear (J) lysates from (E) and (F), showing overexpression of DBC1(1–470)*, in U2OS cells stably expressing DBC1 shRNA.

Author Manuscript
Author Manuscript
Author Manuscript
Author Manuscript

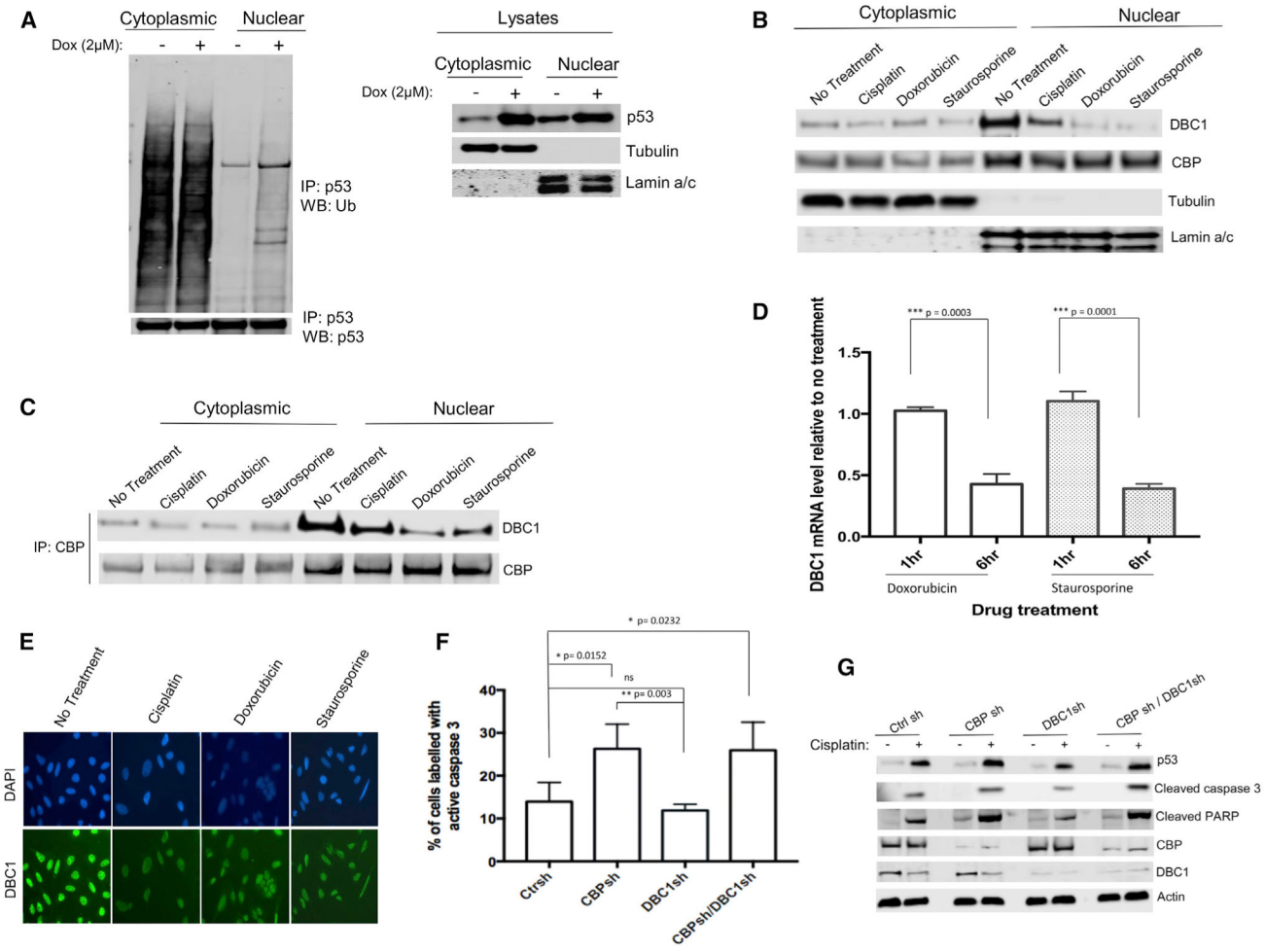

Figure 6. Opposing Roles of CBP and DBC1 in Apoptosis

(A) U2OS cells were untreated or treated with 2 μM doxorubicin, followed by p53 IP (left) from cytoplasmic and nuclear lysates, respectively, followed by immunoblotting. Lysates were calibrated for p53 levels by immunoblotting (right) to allow equal levels of p53 in each IP. See also Figures S4A, S4B, and S5.

(B) U2OS cells were untreated or treated with 2 μM doxorubicin, 25 μM cisplatin, or 1 μM staurosporine for 6 h, followed by immunoblotting of cytoplasmic and nuclear lysates. See also Figure S4C.

(C) CBP IPs from cytoplasmic and nuclear fractions in (B), followed by immunoblotting with CBP and DBC1 antibodies.

(D) U2OS cells were untreated or treated with 2 μM doxorubicin or 1 μM staurosporine for 1 and 6 h, followed by qRT-PCR to determine DBC1 mRNA levels. Graph shows DBC1 mRNA levels relative to no treatment control. Error bars represent mean ± SEM from three independent experiments. RNA level was normalized to GAPDH.

(E) Immunofluorescence of U2OS cells untreated or treated with 25 μM cisplatin, 2 μM doxorubicin, or 1 μM staurosporine for 6 h and stained with DBC1 antibody.

(F) U2OS cells stably expressing control shRNA, CBP shRNA, DBC1 shRNA, or CBP-DBC1 shRNAs were treated with 25 μM cisplatin for 24 h, followed by cell

Author Manuscript Author Manuscript Author Manuscript Author Manuscript

permeabilization, staining with anti-cleaved caspase-3 antibody, and analysis by flow cytometry. Graph shows the percentage of cells with cleaved caspase-3. Error bars represent mean ± SEM from three independent experiments.

(G) U2OS cells stably expressing control, CBP, DBC1, or CBP-DBC1 shRNAs were treated with 25 μM cisplatin for 24 h, followed by cell lysis and immunoblotting with the indicated antibodies. See also Figure S6A.

Author Manuscript
Author Manuscript
Author Manuscript
Author Manuscript

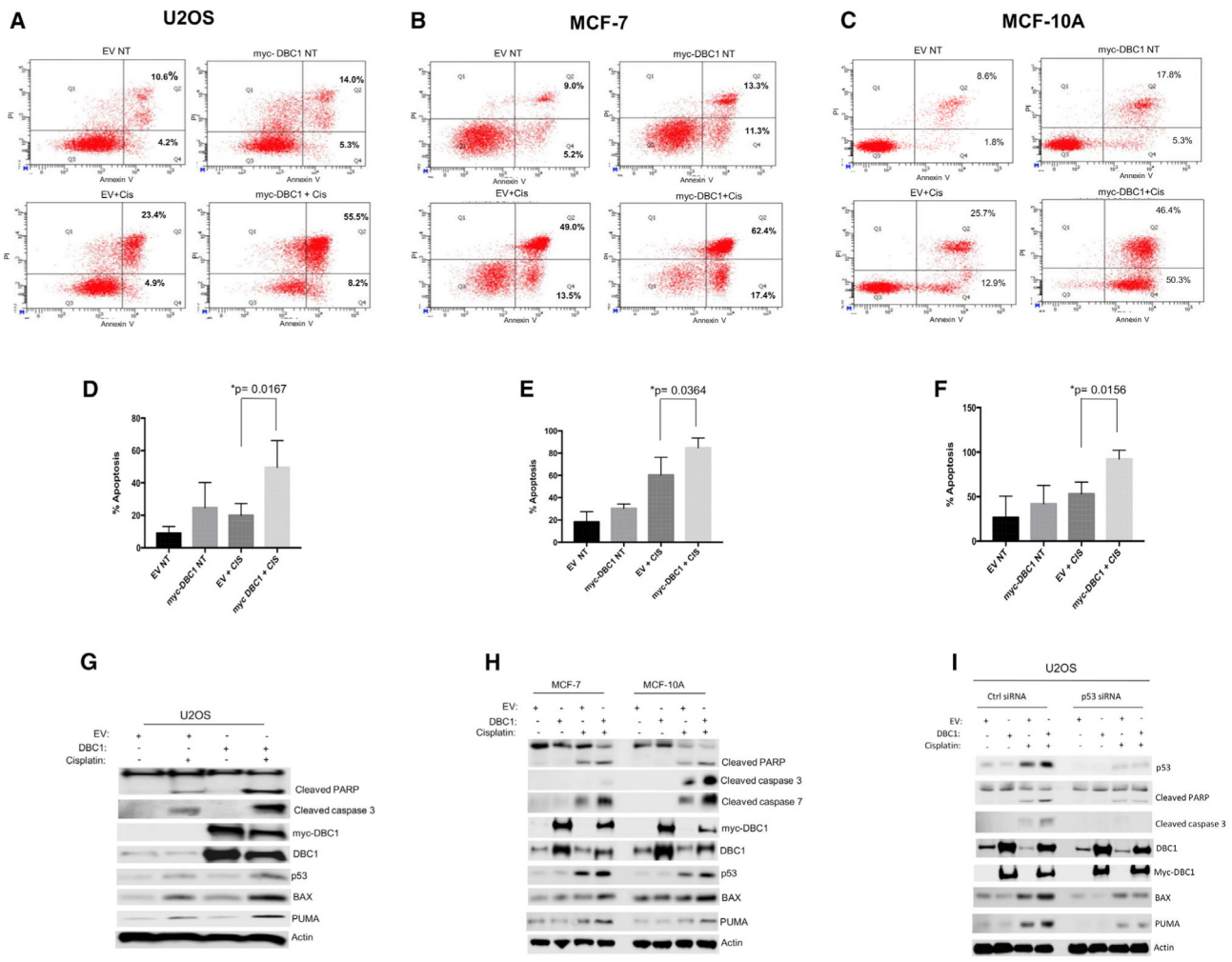

Figure 7. DBC1 Overexpression Promotes p53-Dependent Apoptosis

(A–C) Representative flow cytometry histograms for apoptosis using U2OS cells (A), MCF-7 cells (B), and MCF-10A cells (C). Analysis of apoptosis by flow cytometry of annexin-PI-stained U2OS, MCF-7, and MCF-10A cells transfected with either empty vector or myc-DBC1 and treated with 25 μM cisplatin. Percentages in the Q2 and Q4 quadrants represent the early and late apoptotic populations, resepctively. See also Figure S6B.

(D–F) Quantification of apoptosis measured by flow cytometry from three independent experiments for U2OS cells (D), MCF-7 cells (E), and MCF-10A cells (F) treated as in (A)–(C). Error bars represent mean ± SEM from three independent experiments.

(G–H) U2OS cells (G), MCF-7 cells (H), and MCF-10A cells (H) transfected with either empty vector or myc-DBC1 were treated with 25 μM cisplatin, followed by cell lysis and immunoblotting using the indicated antibodies. (I) U2OS cells were treated with either control siRNA or p53 siRNA, followed by transfection with empty vector or full-length myc-DBC1 plasmids. 24 h before lysis, cells were exposed to 25 μM cisplatin. Lysed cells were subjected to immunoblotting using the indicated antibodies.

Author Manuscript Author Manuscript Author Manuscript Author Manuscript

KEY RESOURCES TABLE

REAGENT or RESOURCE	SOURCE	IDENTIFIER
Antibodies		
Rabbit polyclonal anti-CBP (A-22)	Santa Cruz	Cat. # sc-369; RRID: AB_631006
Mouse monoclonal anti-CBP	Santa Cruz	Cat. # sc-7300; RRID: AB_626817
Rabbit polyclonal anti-DBC1/p30 DBC1	Bethyl	Cat. # A300-432A; RRID: AB_420941
Mouse monoclonal anti-p53 (DO1)	Santa Cruz	Cat. # sc-126; RRID: AB_628082
Rabbit polyclonal anti-p53 (FL393)	Santa Cruz	Cat. # sc-6243; RRID: AB_653753
Goat polyclonal anti-DBC1	Santa Cruz	discontinued
Mouse monoclonal anti-FLAG (M2)	Sigma-Aldrich	Cat. # A2220; RRID:AB_10063035
Rabbit anti-FLAG (TM)	Sigma-Aldrich	Cat. # F7425; RRID:AB_439687
Mouse monoclonal anti-myc clone 4A6	Millipore	Cat. # 16-219; RRID:AB_390197
Mouse monoclonal anti-Ub	Santa Cruz	Cat. # sc-8017; RRID:AB_628423
Mouse monoclonal anti-Ub (VU-1)	Life sensors	Cat. # VU101; RRID:AB_2716558
Rabbit polyclonal anti-cleaved PARP	Cell signaling	Cat. # 9532S; RRID:AB_659884
Rabbit polyclonal anti-cleaved caspase 3	Cell signaling	Cat. # 9661S; RRID:AB_2341188
Rabbit polyclonal anti-cleaved caspase 7	Cell signaling	Cat. # 9491S; RRID:AB_2068144
Rabbit polyclonal anti-BAX	Cell signaling	Cat. # 2772S; RRID:AB_10695870
Rabbit polyclonal anti-PUMA	Cell signaling	Cat. # 12450; RRID:AB_2064551
Rabbit polyclonal anti-actin	Sigma-Aldrich	Cat. # A 2066; RRID:AB_476693
Mouse monoclonal anti-α-tubulin	Sigma-Aldrich	Cat. #T 9026; RRID:AB_477593
Rabbit polyclonal anti-Lamin a/c	Cell signaling	Cat. # 2032S; RRID:AB_2136278
Alexa Fluor 647 Rabbit anti-active caspase 3	BD Biosciences	Cat. #560626; RRID:AB_1727414
Bacterial and Virus Strains		
Mission pLKO.1-puro Non-target control shRNA plasmid	Sigma-Aldrich	SHC016-1EA
GIPZ Non-silencing shRNA lentiviral shRNA control	GE healthcare Dharmacon	RHS4346
Plasmids or siRNA		
siRNA: negative control	Ambion	Cat. # 4636
siRNA: CBP	Ambion	Cat. # 4390829
siRNA: p53	Dharmacon	L-003329-00-0010
siRNA: DBC1	Dharmacon	L-010427-00-0050
ShRNA: GIPZ Human CREBBP (CBP)	Dharmacon	Cat. # RHS4430-200236268
shRNA: DBC1	Sigma-Aldrich	SHCLNG-NM_021174
Chemicals, Peptides, and Recombinant Proteins		
Doxorubicin	Sigma-Aldrich	Sigma D1515
Etoposide	Sigma-Aldrich	Sigma E1383
Cisplatin	Selleck Chemicals	S1166
Staurosporine	Abcam	ab146588
Roche mini complete EDTA free	Roche	Cat. # 11836170001
Cycloheximide	Sigma-Aldrich	Cat # C7698
SeeBlue™ Plus 2 Pre-stained protein standard	Invitrogen™	Cat # LC5925

Author Manuscript Author Manuscript Author Manuscript Author Manuscript

REAGENT or RESOURCE	SOURCE	IDENTIFIER
HiMark™ Pre-stained protein standard	Invitrogen™	Cat # LC5699
Critical Commercial Assays		
MudPIT analysis	Proteomics Core, University of Virginia, Charlottesville, VA, USA.	nes3f@virginia.edu
Deposited Data		
Mass Spec	This study	ProteomeXchange with identifier PRIDE: PXD012673
Experimental Models: Cell Lines		
U2OS	ATCC	ATCC#HTB-96
HEK293T	ATCC	ATCC#CRL-3216
H1299	ATCC	ATCC#CRL-5803
MCF-7	Laboratory of Koblinski	jennifer.koblinski@vcuhealth.org
MCF-10A	Laboratory of Koblinski	jennifer.koblinski@vcuhealth.org
Experimental Models: Organisms/Strains		
E. coli BL21 Gold (DE3)	Thermo Fisher	Cat # 50-125-348
Oligonucleotides		
Table S1	This study	Table S1
Recombinant DNA		
pcDNA 3.0 myc- full length DBC1	Addgene	Cat. # 35096
pcDNA 3.0 myc- DBC1 1-240aa	This study	N/A
pcDNA 3.0 myc-DBC1 1-470aa	This study	N/A
pcDNA 3.0 myc- DBC1 697-923aa	This study	N/A
pcDNA 3.0 FLAG-full length CBP	Shi et al., 2009	N/A
pcDNA 3.0 FLAG-CBP 1-200	Shi et al., 2009	N/A
pcDNA 3.0 FLAG-CBP 1-351	Shi et al., 2009	N/A
pcDNA 3.0 FLAG-CBP1-456	Shi et al., 2009	N/A
pcDNA 3.0 FLAG-CBP 1-616	Shi et al., 2009	N/A
pcDNA 3.0 FLAG-CBP Δ1-665	Shi et al., 2009	N/A
Software and Algorithms		
Prism	GraphPad Software	http://www.graphpad.com/scientific-software/prism/
Scaffold	Scaffold by Proteome Software	http://www.proteomesoftware.com/